Metamaterial-Inspired Decoupling of MIMO Antennas for Wireless Systems

Md. Emdadul Hoque Bhuiyan [1], Md. Mohiuddin Soliman [2], Norsuzlin Mohd Sahar [3,*], Mohammad Tariqul Islam [2,*], and Mohamed Ouda [4]

[1] Department of Electronic and Electrical Engineering, Kyungpook National University, Daegu, South Korea
[2] Department of Electrical, Electronic and Systems Engineering, Faculty of Engineering and Built Environment, Universiti Kebangsaan Malaysia, Bangi-43600, Selangor, Malaysia
[3] Space Science Center (ANGKASA), Universiti Kebangsaan Malaysia, Bangi, Selangor 43600, Malaysia
[4] Department of Telecommunication and Network Engineering, College of Engineering and Technology, University of Doha for Science and Technology, Qatar
Email: mehbhuiyan1@knu.ac.kr (M.E.H.B.); p108446@siswa.ukm.edu.my (M.M.S.); norsuzlin@ukm.edu.my (N.M.S.); tariqul@ukm.edu.my (M.T.I.); mohamed.ouda@udst.edu.qa (M.O.)
*Corresponding author

***Abstract*—This paper reports an innovative technique aimed at diminishing the mutual interference, technically termed 'mutual coupling', between two Microstrip Patch Antenna (MPA) elements. These elements, operating together at 5.8 GHz, are placed in proximity, separated by only 7 mm, which corresponds to approximately 0.14 λ at the operating frequency. The core of our investigation revolves around the strategic placement of various metamaterial structures between these two adjacent Multiple Input Multiple Output (MIMO) elements. The study reveals a striking observation: without the incorporation of metamaterial, the mutual coupling coefficient, denoted as |S21|, stands at −21.7744 dB. However, a transformative shift occurs with the introduction of a specific metamaterial composed of five Circular Complementary Split-Ring Resonator (CSRR) unit cells. This configuration results in a significant enhancement, reducing the |S21| parameter from −21.7744 dB to −43.3581 dB. This significant reduction showcases the effectiveness of our approach. Further examination of the proposed MIMO antenna, integrated with the Circular CSRR metamaterial, unveils a suite of impressive characteristics. Notably, it boasts a reflection coefficient (|S11|) maintained below −10 dB, a noteworthy feat in antenna design. Moreover, the antenna demonstrates a superbly high value of diversity gain, quantified at 9.99999, alongside an exceptionally low Envelope Correlatzicient (ECC), recorded at a minuscule 0.000001. These results demonstrate that the proposed MIMO antenna, enhanced with the circular CSRR metamaterial, effectively reduces mutual coupling while maintaining favorable reflection and diversity performance. The design offers improved isolation, low ECC, and high DG, indicating its suitability for compact, high-efficiency MIMO antenna applications in wireless communication systems.**

***Keywords*—Multiple Input Multiple Output (MIMO), circular CSRR metamaterial, MPA elements, mutual coupling, S-parameters**

Manuscript received October 23, 2025; revised November 19, 2025; accepted November 25, 2025; published March 24, 2026.

I. Introduction

The arrival of 5G communication technology signals the beginning of a revolutionary new age in digital connectivity, one that is characterized by a massive advance in technological development. This new technological frontier is defined by a variety of improvements, including enhanced data rates soaring to new heights, latency reduced to mere fractions, reliability reaching unprecedented levels, cost efficiency becoming a paramount feature, and network capacity expanding to accommodate a massive influx of consumers and a diverse range of applications [1, 2]. This evolution is not taking a linear path; rather, it is exponential, completely transforming the landscape of communication technology. The Multiple Input Multiple Output (MIMO) system is emerging as a beacon of promise amid this technological revolution. MIMO is recognized for its ability to deliver extremely fast data speeds, rock-solid reliability, and greatly reduced latency. It is highly regarded in academic and industrial circles for its capacity to support a large user population, further solidifying its position as an indispensable part of the 5G infrastructure [3]. MIMO is not merely a component of the 5G revolution; rather, it is one of the primary driving forces behind it.

Nevertheless, the development of MIMO antennas has not been without challenges. To achieve high data rates in modern communication systems, antenna arrays and MIMO technology are employed to improve network coverage and capacity. The decoupling analysis is mainly presented for MIMO applications [4–8]. Most of these techniques work by fabricating coplanar structures adjacent to the antenna on the same substrate [9, 10], which increases circuit complexity and further raises the cost and size of the system. These methods still face significant obstacles, the most critical of which is mutual coupling—a phenomenon in which the proximity of antenna elements results in electromagnetic interference,

severely degrading system performance [11]. This challenge becomes even more complex with the extensive use of multiple Radiofrequency (RF) chains, introducing additional logistical and financial burdens.

II. Literature Review

In response to this critical problem, numerous new approaches have been proposed. Notably, a study [3] recommends the use of a neutralization line between two monopole antennas to achieve improvement in isolation better than −19 dB. Electromagnetic Bandgap (EBG) Metamaterial Fractal Loading is another innovative method, demonstrating isolation enhancement of up to −37 dB [11]. Further developments include the integration of five SRR unit cells, which significantly reduce mutual coupling between closely spaced radiating elements, resulting in an improvement of −35 dB at 7.8 GHz [12]. Other advancements include the incorporation of Electromagnetic Bandgap structures combined with ground stubs, which are effective, especially in ultrawideband applications. This configuration achieves S21 < −25 dB, an ECC < 0.01, and a Diversity Gain (DG) > 9.995 [13]. Additional notable strategies discussed in the literature include meta surface-based coupling reduction techniques [14], metamaterial-based isolation enhancement [12], and the utilization of SRR-like structures [15]. These metamaterial-based decoupling techniques have gained significant attention due to their unique electromagnetic properties, which enhance the fundamental parameters of MIMO antennas [16]. One such advancement is the Complementary Split-Ring Resonator (CSRR), created by etching a split-ring resonator into the conducting plane [17]. Another contribution is the implementation of a metamaterial structure to reduce mutual coupling between Vivaldi antenna arrays, leading to improved isolation and the potential for enhanced imaging resolution [18]. Additionally, a new configuration incorporating slots and conducting strips has been shown, through both simulation and measurement, to significantly reduce mutual coupling between adjacent microstrip patch antennas [19].

This study presents a ground-breaking strategy for mitigating the effects of mutual coupling in MIMO antennas by making use of a variety of metamaterial structures composed of CSRR unit cells. The product is a MIMO antenna that has been merged with a Circular CSRR metamaterial. This antenna not only achieves the largest reduction possible in mutual coupling, but it also performs exceptionally well in terms of diversity. With its Circular CSRR metamaterial, this suggested MIMO antenna structure offers a solution that is very effective, in addition to being highly adaptable, for a wide variety of wireless applications. In summary, this research makes a significant contribution to the narrative around 5G. It provides a solution that not only directly addresses the problem of mutual coupling but also improves the overall performance of MIMO antennas. This is a significant advantage. Such advancements will play a critical part in ensuring that the potential of this revolutionary technology is completely realized, opening the way for a future that is more connected, efficient, and technologically sophisticated. As we move deeper into the 5G age, we will continue to move closer to realizing this potential.

III. Materials and Methods

The design and simulation of the proposed MIMO antenna are performed in CST Studio Suite. The antenna is designed at an operational frequency of 5.8 GHz with a dielectric substrate and a conducting ground plane ($W \times L = 44 \times 36$ mm²). The substrate material is FR-4 (lossy) with a relative permittivity of 4.3, a height of 1.6 mm, and a loss tangent of 0.025. The ground plane material is annealed copper with a thickness (t) of 0.035 mm, and the ground plane shares the same width and length as the substrate. First, two MPA elements are constructed on the substrate, having optimized dimensions of Wp = 15 mm and Lp = 12 mm. The width of the feedline (Wf) connected to the patch is 3 mm, and the MPA elements have the same thickness (t) as the ground plane. The edge-to-edge separation (gap) between the MPA elements is 7 mm, which corresponds to approximately 0.14 λ at the operating frequency of 5.8 GHz. The MPA elements are fed using coaxial cables, as shown in Fig. 1. The radii of the outer and inner copper conductors are listed in Table I. The dielectric material between the inner and outer conductors is Teflon (PTFE, lossy) with a permittivity of 2.1. Following this, different metamaterial structures consisting of five CSRR unit cells are inserted between the MPA elements to examine mutual coupling reduction. The Length (Lssr) of the metamaterial structure is 30 mm, and the Width (Wssr) is 6 mm.

In Fig. 2(a), a metamaterial of five Hexagonal CSRR unit cells is utilized to lower the mutual coupling. Variables and dimensions of a hexagonal CSRR unit cell are: Ws = 6mm, Ls = 6 mm, Hg = 0.26 mm, Hf = 0.61 mm, Hl = 2.79 mm, g = 0.28 mm. In Fig. 2(b), a metamaterial consisting of five Square CSRR unit cells are employed to reduce mutual coupling between the MPA elements. Variables and dimensions of a hexagonal CSRR unit cell are: Ws = 6 mm, Ls = 6 mm, Sg = 0.22 mm, g = 0.28 mm, Sf = 0.5 mm, Sl = 2.53 mm, Sh = 3.95 mm. In Fig. 2(c), a metamaterial of five Circular CSRR unit cells are used to compress the mutual coupling. Variables and dimensions of a hexagonal CSRR unit cell are: Ws = 6 mm, Ls = 6 mm, rin = 1.49 mm, rout =1.79 mm, RRin = 2.49 mm, RRout = 2.79 mm, g = 0.28 mm.

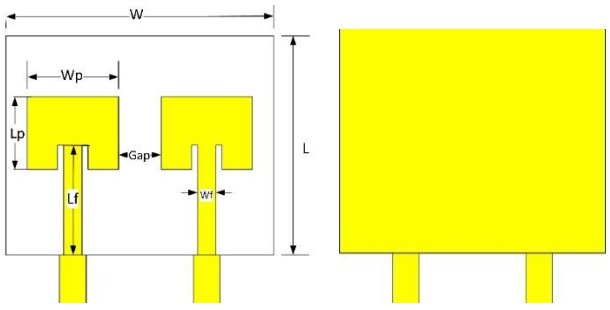

Fig. 1. Basic design of MIMO antenna without metamaterial: (a) front view, (b) bottom view.

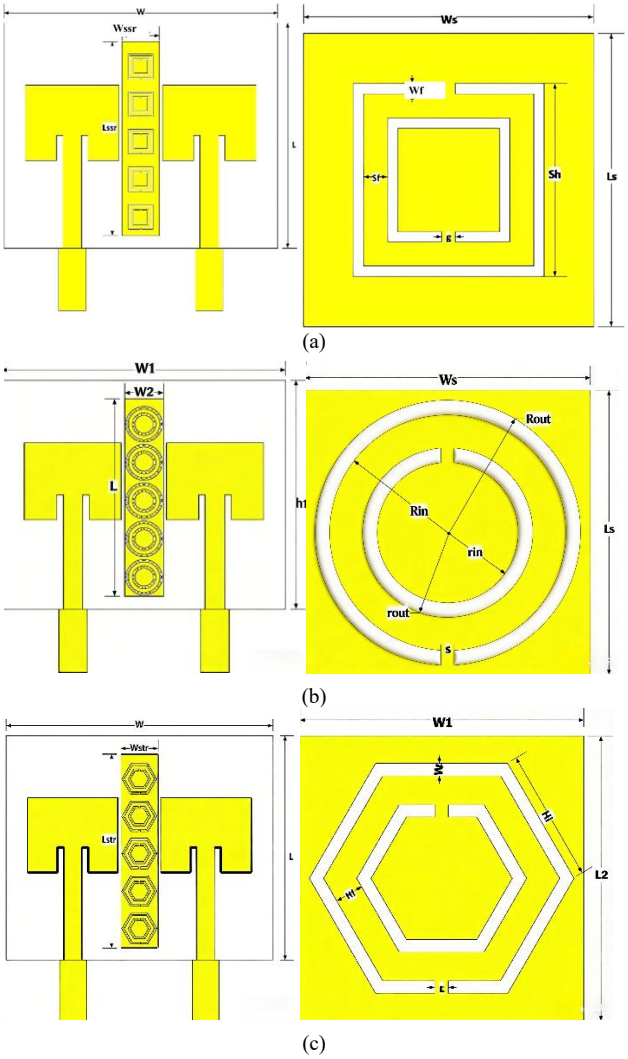

Fig. 2. Design of MIMO antenna: (a) with square CSRR metamaterial, (b) with circular CSRR metamaterial, (c) with hexagonal CSRR metamaterial.

TABLE I. VARIABLES AND DIMENSIONS OF BASIC DESIGN

Variable	Value (mm)	Variable	Value (mm)	Variable	Value (mm)
W	44	WP	15	Lc	10
L	36	Lp	12	teflon	0.635
Subh	1.6	Wf	3	C-outR	2.2
t	0.035	Lf	18	C-inR	2.1

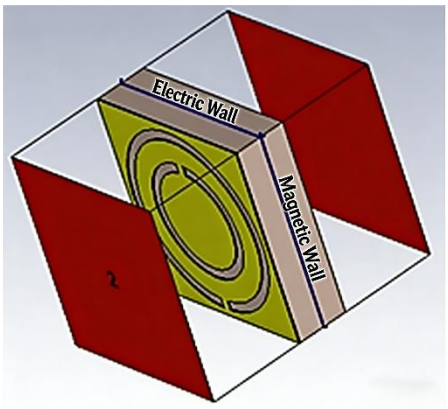

Fig. 3. Design and boundary conditions of a single circular CSRR metamaterial unit cell.

In Fig. 3, a Circular CSRR metamaterial unit cell made up of double circular split rings was designed at the frequency of 5.8 GHz and constructed by implementing the Babinet principle, and CSRR is the negative image of the Split Ring Resonator according to the principle [1]. The behaviour of electromagnetic waves within the metamaterial structure and observing the associated field properties at resonance frequencies.

IV. RESULT AND DISCUSSION

This section presents the performance evaluation of the proposed MIMO antenna. Key parameters, including the reflection coefficient, surface current distribution, radiation pattern, and efficiency, are discussed in detail to assess the impact of the circular CSRR metamaterial on antenna operation and MIMO performance. These results provide insight into how the proposed design enhances isolation, improves diversity metrics, and maintains overall antenna efficiency.

A. S-Parameter

Fig. 4(a) compares the reflection coefficient $|S_{11}|$ for the antenna without metamaterial and with different metamaterial structures. An S11 value below −10 dB is observed both without metamaterial and with the various CSRR-based metamaterials at the operating frequency of 5.8 GHz. In Fig. 4(b), the mutual coupling coefficient |S21| without the metamaterial is −21.7744 dB at 5.8 GHz. With the Circular CSRR metamaterial, $|S_{21}|$ is significantly reduced to −43.3581 dB, yielding an improvement of approximately 22 dB. Hence, we have considered the circular CSRR as the proposed version.

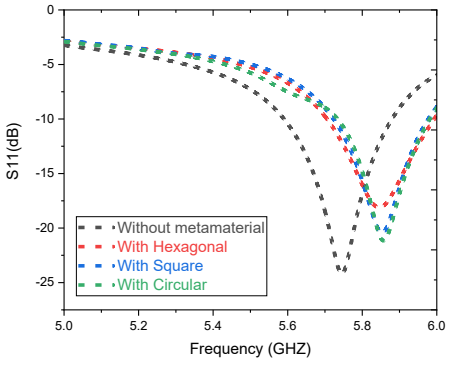

(a)

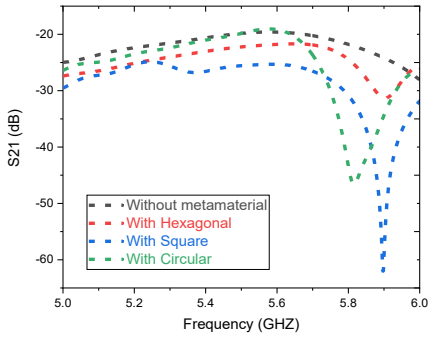

(b)

Fig. 4. S-parameter without metamaterial and with different CSRR metamaterials: (a) S11, (b) S21.

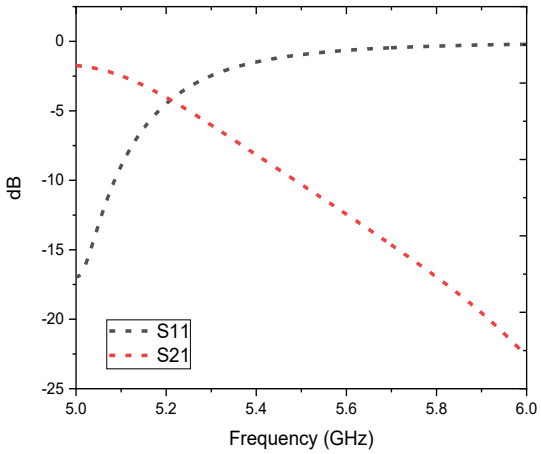

(a)

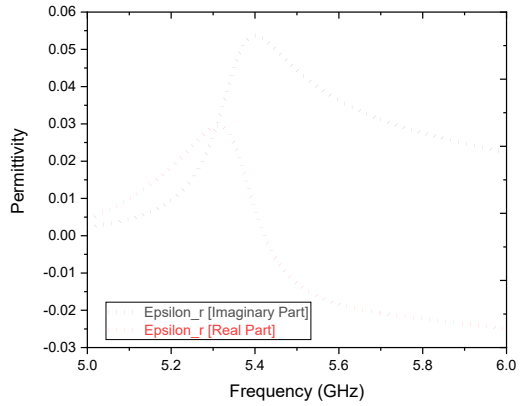

(b)

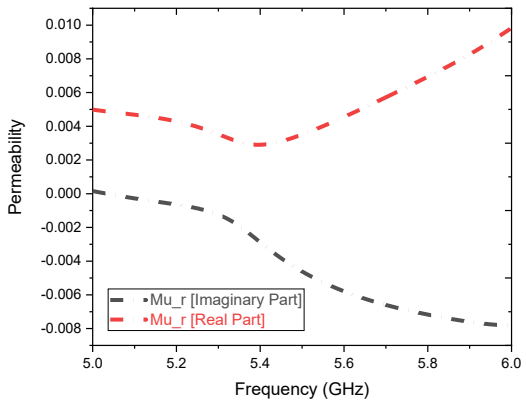

(c)

Fig. 5. A circular CSRR unit cell: (a) S parameters, (b) permittivity, (c) permeability.

Fig. 5(a) depicts the scattering parameters of the circular CSRR unit cell, where the reflection coefficient $|S_{11}|$ approaches 0 dB and the transmission coefficient $|S_{21}|$ is about −18 dB. This result ensures that the unit cell acts as a bandgap process at the resonance frequency, which is applicable in reducing mutual coupling in our proposed work. Figs. 5(b) and 5(c) show the extracted permittivity and permeability of the Circular CSRR unit cell, respectively. The CSRR generates the real part of effective negative permittivity (Ɛ) < 0 instead of effective magnetic permeability (μ) < 0 near the resonance frequency [20, 21]. Accordingly, our results say that the circular CSRR unit cell produces the real part of negative permittivity (Ɛ) < 0 instead of magnetic permeability (μ) < 0 near the resonance frequency.

B. Surface Current Distribution

Fig. 6 illustrates the surface current distributions without and with different metamaterials at the operating frequency of 5.8 GHz. In Fig. 6(a), it is observed that the coupled current on the adjacent radiator is very strong in the absence of a metamaterial. In contrast, Fig. 6(d) shows that the interaction (mutual coupling) between the radiating antennas is significantly reduced after the addition of the Circular CSRR metamaterial.

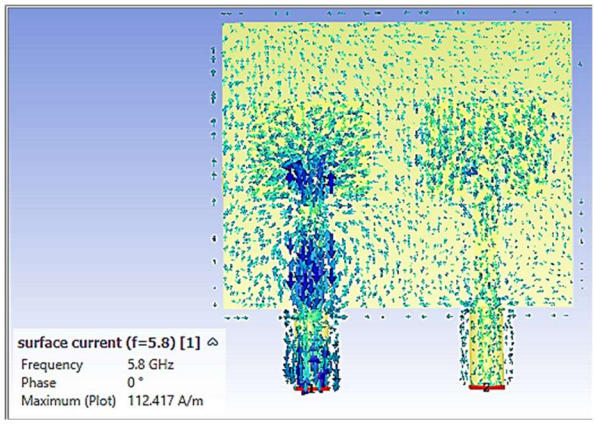

(a)

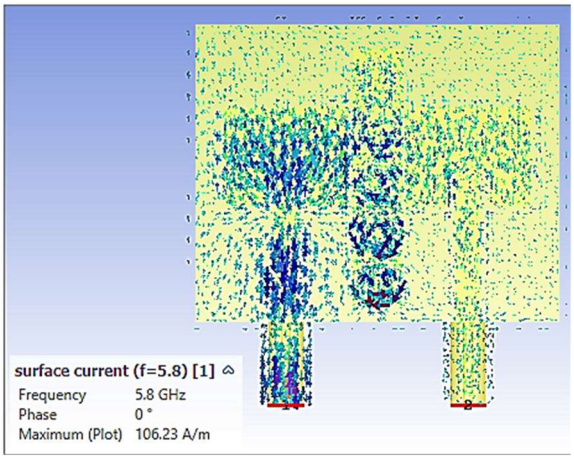

(b)

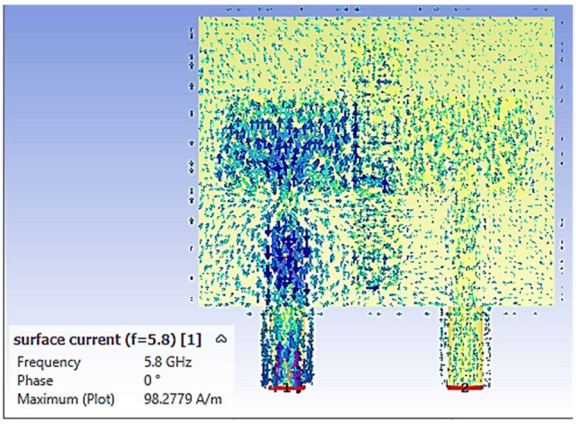

(c)

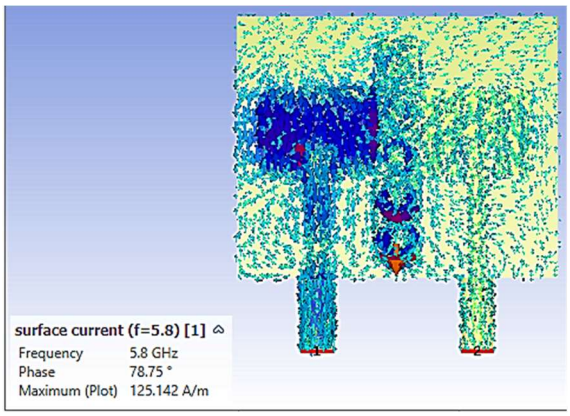

(d)

Fig. 6. Surface current distribution: (a) without metamaterial, (b) with hexagonal CSRR metamaterial, (c) with square CSRR metamaterial, (d) with circular CSRR metamaterial.

C. Radiation Pattern

Fig. 7 illustrates the radiation pattern in the Azimuth and Elevation planes. The radiation pattern represents the directional (angular) dependence of the strength of the radiated waves [22]. Without a metamaterial, the radiation and total efficiencies are −2.545 dB and −2.666 dB, respectively. With the Circular CSRR metamaterial, the radiation efficiency is −2.793 dB, and the total efficiency is −2.938 dB. Additionally, in the Azimuth plane, the angular width is 101.4° with a sidelobe level of −12.1 dB, while in the Elevation plane, the angular width is 60.4° with a sidelobe level of −7.1 dB.

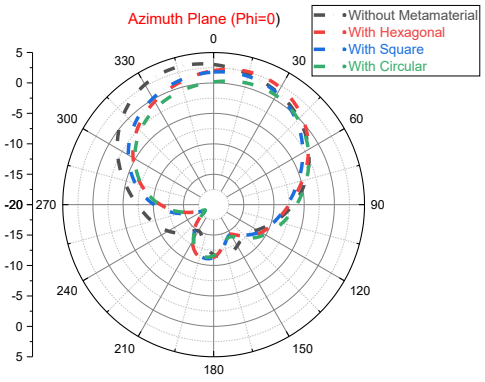

(a)

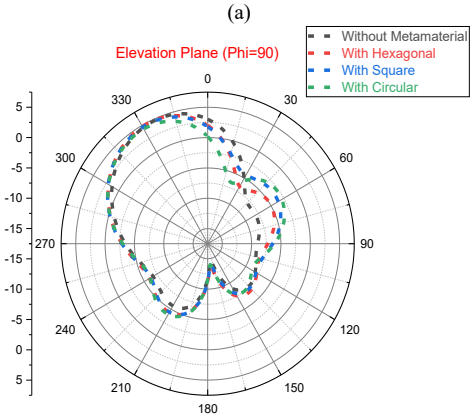

(b)

Fig. 7. Radiation pattern: (a) Azimuth plane, (b) Elevation planes.

D. ECC and DG

Envelope Correlation Coefficient (ECC) is one of the vital parameters to evaluate the performance of a MIMO antenna. A tolerable value of 0.5 or less is considered for a recommended operating MIMO Antenna. Two mathematical expressions are mainly used to calculate the value of ECC; the first one is based on the far-field radiation pattern, and the second one is from the S-parameters of the antenna [13]. Expression of the first one by using far-field radiation patterns [23] is followed by Eq. (1).

$$\mathbf{ECC} = \frac{\left|\int\int_{4\pi}\left(\vec{F}_i(\theta,\emptyset)\right)\times\left(\vec{F}_j(\theta,\emptyset)\right)d\Omega\right|^2}{\iint_{4\pi}\left|\left(\vec{F}_i(\theta,\emptyset)\right)\right|^2 d\Omega \iint_{4\pi}\left|\left(\vec{F}_j(\theta,\emptyset)\right)\right|^2 d\Omega} \quad (1)$$

Expression of the second one by using the scattering parameters [24] as follows: Eq. (2).

$$\mathbf{ECC} = \frac{\left|S_{11}^* S_{12} + S_{21}^* S_{22}\right|^2}{\left(1-|S_{11}|^2-|S_{21}|^2\right)\left(1-|S_{21}|^2-|S_{12}|^2\right)} \quad (2)$$

Diversity Gain (DG) is another fundamental MIMO performance indicator. A DG close to 10dB is recommended for an operational MIMO antenna [25]. DG can be calculated using the following formula [26]; Fig. 8 shows the simulated results of ECC and DG.

$$\mathbf{DG} = \mathbf{10}\left(\sqrt{\mathbf{1}-(\mathbf{ECC})^2}\right) \quad (3)$$

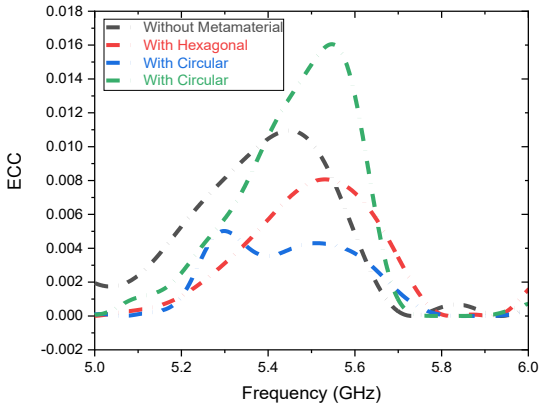

(a)

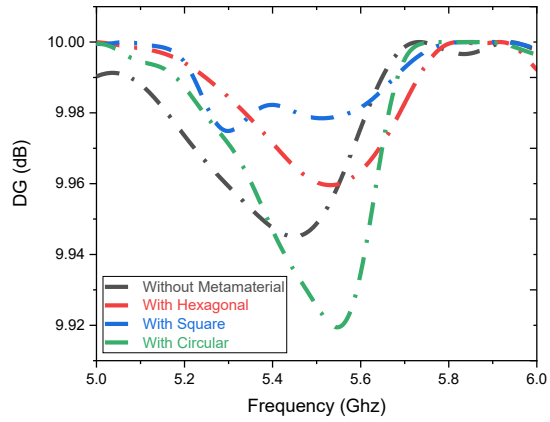

(b)

Fig. 8. Simulated ECC and DG without metamaterial and with different CSRR metamaterials: (a) Envelope Correlation Coefficient (ECC), (b) Diversity Gain (DG).

Table II includes the power simulated, the power radiated, the VSWR, and some far-field parameters. The ideal value of simulated power is 0.5, and the proposed antennas with every metamaterial provide the exact value of 0.5 as indicated in Table II. The coaxial feed technique is one of the most common techniques used for feeding microstrip patch antennas to get impedance matching [27]. Accordingly, a reference impedance value of almost 50 Ω is achieved in every antenna after the simulation.

TABLE II. SOME OTHER ANTENNA PARAMETERS

Design	Power Simulated	Power Radiated (dB)	VSWR	Dir. (dBi)	Gain (dB)	Rad. Eff. (dB)	Tot. Eff. (dB)
Without Metamaterial	0.4999	−5.676	1.338	7.284	4.739	−2.545	−2.666
With a Hexagonal CSRR metamaterial	0.5	−5.719	1.373	7.414	4.830	−2.584	−2.709
With Square CSRR metamaterial	0.5	−5.682	1.39	7.297	4.746	−2.551	−2.673

V. DISCUSSION

Table III describes the comparison of some key parameters that specify the mutual coupling reduction and diversity performance of the MIMO antenna without and with different metamaterial structures. With every metamaterial, the performance meets the requirements of a recommended MIMO antenna. But with Circular CSRR metamaterial, the highest mutual coupling reduction from –21.7744 dB to –43.3581 dB with the highest diversity performance (DG = 9.99999 dB and ECC = 0.000001) is gained.

The results of the proposed antenna with Circular CSRR metamaterial are compared to some recent published works in Table IV. As a result, the proposed work has the best performance of all of them. Table IV presents a comparison of the proposed MIMO antenna with several recently published works in terms of mutual coupling (|S21|), ECC, and DG. It is evident that the proposed design with the Circular CSRR metamaterial significantly outperforms previous techniques, achieving the lowest mutual coupling of −43 dB, which is substantially better than other methods ranging from −15 dB to −34 dB. The ECC value is exceptionally low (< 0.00001), indicating near-ideal diversity performance, while the DG exceeds 9.9999 dB, highlighting excellent MIMO channel reliability. These results confirm that the proposed metamaterial approach provides superior isolation and enhanced MIMO performance compared to existing techniques.

TABLE III. COMPARISON OF SOME KEY PARAMETERS

Design	Mutual Coupling |S21| in dB	DG in dB	ECC
Without Metamaterial	−21.7744	9.99741	0.00051
With a Hexagonal CSRR metamaterial	−24.4504	9.99952	0.00009
With Square CSRR metamaterial	−30.8583	9.99965	0.00006
With Circular CSRR metamaterial	−43.3581	9.99999	0.000001

TABLE IV. COMPARISON WITH SOME RECENTLY PUBLISHED WORKS

Ref.	Techniques	Mutual Coupling |S21| in dB	ECC	DG in dB
[5]	Split-Ring Resonator (SRR)	< −34	< 0.1	> 9
[6]	Ground Stub and EBG	< −25	< 0.1	> 9.99
[7]	Metasurface-based Decoupling	< −25	< 0.4	–
[8]	Metamaterial based	< −20	< 0.1	> 9
[9]	Split-Ring Resonator (SRR)	< −18	< 0.004	> 9.94
[21]	Hybrid Technique	< −28	< 0.04	> 9.9
[22]	F-Shaped stubs	< −20	< 0.04	7.4
[23]	CMA and Cross-shaped Stub	< −15	< 0.05	> 9.97
[24]	Parasitic Decoupling	< −20	< 0.02	–
[25]	Resistor-loaded paired parallel-coupled resonators	< −17	< 0.01	> 9.99
Proposed Work	With Circular CSRR metamaterial	< − 43	< 0.00001	> 9.9999

VI. CONCLUSION

In this paper, a metamaterial-based technique is employed to overcome the mutual coupling effect of a MIMO antenna, and a comparative analysis without and with different metamaterial structures is carried out. With the Circular CSRR metamaterial, the highest mutual coupling reduction and diversity performance are achieved.

Thus, the fundamental parameters for the MIMO antenna, like mutual coupling |S21|, ECC, and DG, acknowledge that the proposed antenna with Circular CSRR metamaterial can be a good candidate for the MIMO antenna system.

CONFLICT OF INTEREST

The authors declare no conflict of interest.

AUTHOR CONTRIBUTIONS

Md. Emdadul Hoque Bhuiyan: Conceptualization, methodology, data analysis, and initial manuscript drafting Md Mohiuddin Soliman: Simulation, validation, result interpretation, and manuscript revision; Norsuzlin Mohd Sahar: Supervision, technical guidance, and critical manuscript review; Mohammad Tariqul Islam: Project administration, resources, and final manuscript approval Mohamed Ouda: Technical support, theoretical insights, and proofreading; all authors had approved the final version.

FUNDING

The authors acknowledged the Fundamental Research Grants Scheme (FRGS) Grant No. FRGS/1/2022/TK07/UKM/02/23, funded by the Ministry of Higher Education (MOHE), Malaysia. The research reported in this publication, was supported by the Qatar Research Development and Innovation Council [ARG010504-230068]. The content is solely the responsibility of the authors and does not necessarily represent the official views of the Qatar Research Development and Innovation Council.

REFERENCES

[1] J. G. Andrews *et al*., "What will 5G be?" *IEEE Journal on Selected Areas in Communications*, vol. 32, no. 6, pp. 1065–1082, Jun. 2014.

[2] M. L. Attiah, A. A. M. Isa, Z. Zakaria, M. K. Abdulhameed, M. K. Mohsen, and I. Ali, "A survey of mmWave user association mechanisms and spectrum sharing approaches: An overview, open issues and challenges, future research trends," *Wireless Netw*., vol. 26, no. 4, pp. 2487–2514, May 2020.

[3] S. W. Su, C. T. Lee, and F. S. Chang, "Printed MIMO-antenna system using neutralization-line technique for wireless USB-dongle applications," *IEEE Transactions on Antennas and Propagation* vol. 60, no. 2, pp. 456–463, Feb. 2012.

[4] A. K. Biswas and U. Chakraborty, "Reduced mutual coupling of compact MIMO antenna designed for WLAN and WiMAX applications," *International Journal of RF and Microwave Computer-Aided Engineering*, vol. 29, no. 3, e21629, 2019.

[5] P. Das, C. Saha, and K. Mandal, "Mutual coupling and RCS reduction of MIMO antenna using a hybrid technique," presented at the 2022 IEEE Wireless Antenna and Microwave Symposium (WAMS), 2022, pp. 1–5.

[6] F. K. Khalili, M. A. Honarvar, M. N. Moghadasi, and M. Dolatshahi, "Gain enhancement and mutual coupling reduction of multiple-intput multiple-output antenna for millimeter-wave applications using two types of novel metamaterial structures," *International Journal of RF and Microwave Computer-Aided Engineering*, vol. 30, no. 1, e22006, 2020.

[7] M. Mishra, S. Chaudhuri, R. S. Kshetrimayum, and H. Chel, "Low mutual coupling six-port planar antenna for the MIMO applications," *International Journal of RF and Microwave Computer-Aided Engineering*, vol. 30, no. 12, e22439, 2020.

[8] F. Urimubenshi, D. B. Konditi, J. de Dieu Iyakaremye, P. M. Mpele, and A. Munyaneza, "A novel approach for low mutual coupling and ultra-compact two port MIMO antenna development for UWB wireless application," *Heliyon.*, vol. 8, no. 3, 2022.

[9] X. Sun and M. Cao, "Mutual coupling reduction in an antenna array by using two parasitic microstrips," *AEU-International Journal of Electronics and Communications*, vol. 74, pp. 1–4, 2017.

[10] X.-J. Zou, G.-M. Wang, Y.-W. Wang, and B.-F. Zong, "Mutual coupling reduction of quasi-Yagi antenna array with hybrid wideband decoupling structure," *AEU-International Journal of Electronics and Communications*, vol. 129, 153553, 2021.

[11] M. Alibakhshikenari, M. Khalily, B. S. Virdee, C. H. See, R. A. Abd-Alhameed, and E. Limiti, "Mutual coupling suppression between two closely placed microstrip patches using EM-bandgap metamaterial fractal loading," *IEEE Access*, vol. 7, pp. 23606–23614, 2019.

[12] A. Iqbal, O. A Saraereh, A. Bouazizi, and A. Basir, "Metamaterial-based highly isolated MIMO antenna for portable wireless applications," *Electronics*, vol. 7, no. 10, p. 267, Oct. 2018.

[13] A. Khan, "Mutual coupling reduction using ground stub and EBG in a compact wideband MIMO-antenna," *IEEE Access*, vol. 9, 2021.

[14] Z. Wang, C. Li, Q. Wu, and Y. Yin, "A metasurface-based low-profile array decoupling technology to enhance isolation in MIMO antenna systems," *IEEE Access*, vol. 8, pp. 125565–125575, 2020.

[15] S. Kharche, G. Reddy, J. Mukherjee, and R. Gupta, "Mutual coupling reduction using variable length SRR like structure in ultra-wideband MIMO antennas," presented at the 2015 IEEE MTT-S International Microwave and RF Conference (IMaRC), IEEE, 2015, pp. 136–139.

[16] T. Shabbir *et al*., "16-port non-planar MIMO antenna system with Near-Zero-Index (NZI) metamaterial decoupling structure for 5G applications," *IEEE Access*, vol. 8, pp. 157946–157958, 2020.

[17] M. K. T. Al-Nuaimi and W. G. Whittow, "Compact microstrip band stop filter using SRR and CSSR: Design, simulation and results," presented at the Fourth European Conference on Antennas and Propagation, IEEE, 2010, pp. 1–5.

[18] A. Ahmed, V. Kumari, and G. Sheoran, "Reduction of mutual coupling in antenna array using metamaterial surface absorber," *AEU−International Journal of Electronics and Communications*, vol. 160, 154519, Feb. 2023.

[19] A. Emadeddin, S. Shad, Z. Rahimian, and H. R. Hassani, "High mutual coupling reduction between microstrip patch antennas using novel structure," *AEU−International Journal of Electronics and Communications*, vol. 71, pp. 152–156, Jan. 2017.

[20] F. Falcone, T. Lopetegi, J. D. Baena, R. Marques, F. Martin, and M. Sorolla, "Effective negative-/spl epsiv/ stopband microstrip lines based on complementary split ring resonators," *IEEE Microwave and Wireless Components Letters*, vol. 14, no. 6, pp. 280–282, Jun. 2004.

[21] N. Ida, *Engineering Electromagnetics*, Springer International Publishing Switzerland, 2015.

[22] F. Falcone *et al*., "Babinet principle applied to the design of metasurfaces and metamaterials," *Physical Review Letters*, vol. 93, no. 19, 197401, 2004.

[23] C. A. Balanis, Antenna Theory: Analysis and Design, John Wiley and Sons, 2016.

[24] M. S. Sharawi, *Printed MIMO Antenna Engineering*, Artech House, 2014.

[25] N. Malekpour and M. A. Honarvar, "Design of high-isolation compact MIMO antenna for UWB application," *Progress in Electromagnetics Research C*, vol. 62, pp. 119–129, 2016.

[26] G. Saxena, P. Jain, and Y. K. Awasthi, "High diversity gain MIMO-antenna for UWB application with WLAN notch band characteristic including human interface devices," *Wireless Personal Communications*, vol. 112, pp. 105–121, 2020.

[27] S. Blanch, J. Romeu, and I. Corbella, "Exact representation of antenna system diversity performance from input parameter description," *Electronics Letters*, vol. 39, no. 9, pp. 705−707, 2003.